Polysaccharide from *Angelica sinensis* protects H9c2 cells against oxidative injury and endoplasmic reticulum stress by activating the ATF6 pathway

Xiaowei Niu[1,*], Jingjing Zhang[2,*], Chun Ling[3,*], Ming Bai[4,5], Yu Peng[4,5], Shaobo Sun[6], Yingdong Li[6] and Zheng Zhang[4,5] (iD)

Abstract

Objectives: *Angelica sinensis* exerts various pharmacological effects, such as antioxidant and anti-apoptotic activity. This study aimed to investigate the active ingredients in *A. sinensis* with antioxidant properties and whether *A. sinensis* polysaccharide (ASP) protects H9c2 cells against oxidative and endoplasmic reticulum (ER) stress.

Methods: The ingredients of *A. sinensis* and their targets and related pathways were determined using web-based databases. Markers of oxidative stress, cell viability, apoptosis, and ER stress-related signalling pathways were measured in H9c2 cells treated with hydrogen peroxide (H_2O_2) and ASP.

Results: The ingredient–pathway–disease network showed that *A. sinensis* exerted protective effects against oxidative injury through its various active ingredients on regulation of multiple pathways. Subsequent experiments showed that ASP pretreatment significantly decreased H_2O_2-induced cytotoxicity and apoptosis in H9c2 cells. ASP pretreatment inhibited H_2O_2-induced reactive oxygen species generation, lactic dehydrogenase release, and malondialdehyde

[1]The First School of Clinical Medicine, Lanzhou University, Lanzhou, Gansu, China
[2]Baiyin Second People's Hospital, Baiyin, Gansu, China
[3]The First People's Hospital of Chuzhou, Chuzhou, Anhui, China
[4]Department of Cardiology, the First Hospital of Lanzhou University, Lanzhou, Gansu, China
[5]Gansu Key Laboratory of Cardiovascular Disease, Lanzhou, Gansu, China

[6]Key Lab of Prevention and Treatment for Chronic Disease, Traditional Chinese Medicine of Gansu Province, Lanzhou, Gansu, China
*These authors contributed equally to this work.

Corresponding author:
Zheng Zhang, Department of Cardiology, the First Hospital of Lanzhou University, No. 1, Donggang West Road, Lanzhou, Gansu 730000, China.
Email: zhangccu@yeah.net

production. ASP exerted beneficial effects by inducing activating transcription factor 6 (ATF6) and increasing ATF6 target protein levels, which in turn attenuated ER stress and increased antioxidant activity.

Conclusions: Our findings indicate that ASP, a major water-soluble component of *A. sinensis*, exerts protective effects against H_2O_2-induced injury in H9c2 cells by activating the ATF6 pathway, thus ameliorating ER and oxidative stress.

Introduction

Oxidative stress (OS) is a well-known factor that promotes apoptosis, and is implicated in the pathophysiology of several cardio-vascular diseases, such as ischaemia/reperfusion injury, atherosclerosis, heart failure, and hypertension.[1–3] The endoplasmic reticulum (ER) plays an important role in maintaining intracellular homeostasis when cells are subjected to a variety of environmental and physiological stresses. OS is usually associated with increased formation of reactive oxygen species (ROS), which disturb cellular redox balance and homeostasis of the protein-folding environment of the ER, leading to ER stress.[4,5] To restore homeostasis of the ER, cells activate unfolded protein response (UPR) signalling pathways. These pathways are regulated by three primary ER-resident transducers called activating transcription factor 6 (ATF6), inositol-requiring enzyme 1α (IRE1α), and pancreatic eIF2-alpha kinase (PERK). ATF6, a 90-kDa glycoprotein (p90 ATF6), is an important transcriptional activator during ER stress.[6] In the presence of misfolded proteins in the ER, the fully form of ATF6 shuttles to the Golgi apparatus, where it undergoes cleavage into its active 50-kDa form (p50 ATF6). Active p50 ATF6 then translocates into the nucleus and activates numerous genes encoding ER chaperones.[6] IRE1α is a kinase and RNase that mediates selective splicing of X-box binding protein 1 (*XBP1*) mRNA.[7] The spliced *XBP1* mRNA encodes an active transcription factor that induces expression of genes encoding ER-associated degradation components.[7] PERK stimulates phosphorylation of eukaryotic translation initiation factor 2α to reduce protein synthesis.[8] The UPR signalling pathways function as protective responses in the early stage of cellular injury. However, under severe conditions, UPR activation is not sufficient to restore normal ER function, which subsequently results in activation of apoptosis.[6–8] The pro- and anti-apoptotic effects of the UPR are associated with the three ER transmembrane proteins of the ER, inducing expression of distinct sets of genes.[9] Therefore, differential modulation of each UPR pathway may be an attractive therapeutic strategy for treating cardiovascular diseases.[9] Several studies have shown that activation of ATF6 increases ER-resident protein expression to avoid the toxic effects of misfolded proteins, including 78-kDa glucose-regulated protein

(GRP78),[10] 94-kDa glucose-regulated protein (GRP94),[11] and protein disulphide isomerase family A, member 6 (PDIA6).[12] Additionally, activation of ATF6 also induces antioxidative stress genes encoding proteins outside the ER, such as catalase (CAT).[13] These studies suggest that the ATF6 branch of UPR has an important protective function against ER stress and oxidative damage.[14]

The root of *Angelica sinensis* (Oliv.) Diels (Umbelliferae), known as Danggui in Chinese, has been used as a tonic agent in China for several years.[15] Accumulating evidence obtained from experimental and clinical studies has highlighted the beneficial roles of *A. sinensis* in treating OS-related diseases.[15] Our previous study showed that an ultra-filtration extract of Danggui Buxue Decoction, a medicinal formula primarily containing *A. sinensis*, protected neonatal rat cardiomyocytes from hydrogen peroxide (H_2O_2)-induced injury by exerting antioxidant and anti-apoptotic effects.[16] Studies have been conducted to identify the active ingredients associated with the antioxidant effects of *A. sinensis*.[15] However, completely determining different components in *A. sinensis* through traditional experimental methods is difficult. A functional network analysis has been proposed to examine the relationship between this herb and its targets and grouped pathways.[17–20] Several cancer studies have established the roles of network analysis in identifying active ingredients and their molecular mechanisms.[19,20]

Therefore, we hypothesized that network analysis using data obtained from publicly available databases will help in systematically understanding the antioxidant effects of *A. sinensis*. *A. sinensis* polysaccharide (ASP), which is the primary water-soluble component of *A. sinensis*, was chosen for further experimental validations. Additionally, we determined the effect of ASP on ER stress and UPR pathways in H_2O_2-treated H9c2 cells.

Materials and methods

Candidate targets associated with OS injury

Candidate targets associated with OS injury were determined using the Comparative Toxicogenomics Database[21] and Open Targets Platform.[22] Known and predicted protein targets associated with OS injury were used as candidate targets. We also used PolySearch,[2] an online text-mining system, to identify reliable targets associated with OS injury.[23] Functional enrichment analysis of the screened targets was performed using Kyoto Encyclopedia of Genes and Genomes (KEGG) pathway analysis, which is available in the Database for Annotation, Visualization and Integrated Discovery (DAVID) v6.8.[24]

Determination of active ingredients in A. sinensis and their targets

Ingredients in *A. sinensis* and their potential targets were determined using the Traditional Chinese Medicine Integrative Database,[18] Bioinformatics Analysis Tool for Molecular mechANism of Traditional Chinese Medicine,[17] and PolySearch[2] tool. These targets were then analysed using KEGG pathway analysis that is available in the Database for Annotation, Visualization and Integrated Discovery. Pathways with a false discovery rate of $P < 0.05$ were considered significant.

Network construction and analysis

Active ingredients in *A. sinensis* were identified if their targets were enriched in the same pathways as OS injury-related candidate targets involved. An ingredient–pathway–disease network was constructed

using Cytoscape software (Version 3.4.0, Cytoscape software, San Diego, CA, USA).

Experimental validation

The rat embryonic ventricular myocardial cell line H9c2 (China Center for Type Culture Collection; Beijing, China) was used to examine the effects of ASP in an *in vitro* experiment. H9c2 cells were cultured in high-glucose Dulbecco's modified eagles medium (HyClone Laboratories, Logan, UT, USA) containing 10% newborn calf serum (Gibco, Auckland, New Zealand) and antibiotics (100 U/mL penicillin and 100 μg/mL streptomycin). H9c2 cells were treated with H_2O_2 and/or ASP (purity ≥90%; Solarbio, Beijing, China) after they reached 80% confluence.

Cell viability assay

H9c2 cells were seeded in 96-well plates (density, 1×10^4 cells/well) and were treated with ASP (0–100 μg/mL) for 4 hours or H_2O_2 (0–400 μM) for 2–8 hours at 37°C in a humidified chamber. Cell viability was measured using the 3-(4,5-dimethylthiazol-2-yl)-2,5-diphenyl-2H-tetrazolium bromide (MTT) assay (Solarbio). Briefly, MTT solution (final concentration, 0.5 mg/mL) was added to each well, and the cells were incubated at 37°C for 4 hours. Culture supernatant was then removed, and 150 μL dimethylsulfoxide was added to each well to dissolve formazan crystals. Optical density (OD) of each well was measured at 490 nm by using an infinite M200PRO microplate reader (Tecan, Männedorf, Switzerland). Cell viability was calculated using the following formula: experimental OD value/control OD value × 100.

OS analysis

OS was determined by analysing intracellular ROS production and malondialdehyde (MDA) and lactate dehydrogenase (LDH) levels after treatment with H_2O_2 and/or ASP. ROS generation in H9c2 cells was determined by performing flow cytometric analysis with an ROS assay kit (Beyotime, Shanghai, China). Briefly, H9c2 cells were harvested after treatment, washed twice with phosphate-buffered saline (PBS), incubated with 2,7-dichlorofluorescein diacetate (final concentration, 10 μM) diluted in a serum-free medium for 30 minutes, and washed three times with PBS. ROS levels in H9c2 cells were measured using a FACSVerse flow cytometer (BD Biosciences, San Jose, CA, USA). MDA and LDH levels were determined using commercially available detection kits (Jiancheng, Nanjing, Jiangsu, China) according to respective kit instructions.

Detection of apoptosis

Apoptosis was evaluated by performing flow cytometric analysis and Hoechst 33342 staining. For performing flow cytometric analysis, the cells were washed twice with PBS and suspended in 100 μL binding buffer containing 5 μL annexin V-fluorescein isothiocyanate (FITC) and 5 μL propidium iodide (PI) (BD Biosciences) in the dark at room temperature. After 15 minutes, the cell suspensions were immediately analysed using a FACSVerse flow cytometer. Percentages of apoptotic cells were calculated as the ratio of annexin V-positive cells to the total cell population × 100. Hoechst 33342 staining (Beyotime) was performed to qualitatively analyse apoptotic cells. After ASP and/or H_2O_2 treatment, H9c2 cells were incubated with 10 μL 1× Hoechst 33342 at 37°C for 10 minutes, washed three times with PBS, and visualized using Olympus IX71 fluorescence microscopy (Olympus, Tokyo, Japan). Additionally, morphological changes in the cells were observed using the Olympus IX71 inverted microscope and photomicrographs were obtained at 10× magnification.

Small interfering RNA transfection

H9c2 cells were seeded in 24-well plates (4×10^4 cells/well). After reaching approximately 50% confluence, the cells were transfected with a small interfering RNA (siRNA) against Atf6 or a non-targeting siRNA using Lipofectamine 2000 (Invitrogen Corporation, Carlsbad, CA, USA), according to the manufacturer's instructions. The sequence of the Atf6 siRNA (siAtf6; Genepharma, Shanghai, China) was as follows: sense, 5'-GUGUGA CUAAACCUGUUCUTT-3' and antisense, 5'-AGACUGAGAACUAGACAACTT-3'. The sequence of the non-targeting siRNA (Genepharma) was as follows: sense, 5'-UUCUCCGAACGUGUCACGUTT-3' and antisense, 5'-ACGUGACACGUUCGGAG AATT-3'. To assess the specific silencing effect of siAtf6, ATF6 protein expression was detected by immunoblot analysis.

Quantitative real-time RT-PCR

Total cellular RNA was extracted using Trizol reagent (Invitrogen) and the reverse transcript reaction was performed using PrimeScript RT reagent Kit (Takara Biotechnology, Dalian, China). The cDNA product was then subjected to quantitative real-time RT-PCR (qRT-PCR) analysis on a LightCycle 480 system (Roche Diagnostics, Burgess Hill, UK). The primers used were as below: for Atf6, 5'-CAGCAAAGACCATCATCATTCA G-3' and 5'-TTAGTCACACACAGTTTT CCGTTC-3'; for Cat, 5'-CTTTGAGGTC ACCCACGATATT-3' and 5'-GTGGGTT TCTCTTCTGGCTATG-3'; and for β-actin, 5'-TGCTATGTTGCCCTAGACT TCG-3' and 5'-GTTGGCATAGAGGTCT TTACGG-3'. Reactions were performed in a 20 μL volume containing 10 μL $2 \times$ SYBR Premix Ex Taq II (Takara Biotechnology), 0.8 μL forward primer, 0.8 μL reverse primer, 2.0 μL cDNA, and 6.4 μL dH$_2$O. The qRT-PCR conditions were 95°C for 30 s followed by 40 cycles with the following settings: 95°C for 5 s, 60°C for 25 s, and 72°C for 30 s. Relative expressions were calculated with normalization to β-actin values by using the $2^{-\Delta\Delta Ct}$ method.[25]

Western blot analysis

H9c2 cells were washed twice with cold PBS and lysed in RIPA buffer (Solarbio), 1% phenylmethylsulfonyl fluoride (Solarbio), and 1% phosphatase inhibitor cocktail (Solarbio). Cell lysates were clarified by centrifugation at $13,000 \times g$ for 10 minutes at 4°C. Protein concentrations were determined using a bicinchoninic acid protein assay kit (Solarbio). Samples were mixed with sodium dodecyl sulphate-polyacrylamide gel electrophoresis loading buffer (Solarbio) and boiled for 10 minutes. Samples were then separated by sodium dodecyl sulphate-polyacrylamide gel electrophoresis and transferred onto polyvinylidene fluoride membranes. The membranes were blocked for 2 hours in 5% skim milk and incubated overnight at 4°C with primary antibodies against Bax (Abcam, Cambridge, UK), Bcl-2 (R&D Systems, Minneapolis, MN, USA), C/EBP homologous protein (CHOP; Cell Signaling, Danvers, MA, USA), pro-Caspase-12 (Proteintech Group, Chicago, IL, USA), cleaved Caspase-12 (Proteintech Group), cleaved Caspase-3 (Cell Signaling), GRP78 (Abcam), GRP94 (Abcam), PDIA6 (Abcam), CAT (Proteintech Group), ATF6 (Proteintech Group), PERK (Proteintech Group), phospho-PERK (Beyotime), IRE1α (Novus Biologicals, Littleton, CO, USA), phospho-IRE1α (Novus Biologicals), and glyceraldehyde-3-phosphate dehydrogenase (GAPDH) (ImmunoWay, Plano, TX, USA). The anti-ATF6 antibody specifically detects endogenous p90 and p50 ATF6 in cardiomyocytes.[13] The membranes were then incubated with horseradish peroxidase-conjugated secondary antibody for 2 hours at 4°C and were examined using Immobilon

Western Chemiluminescent HRP Substrate (Millipore, Billerica, MA, USA). Gel images were obtained using a Universal Hood II Imager (Bio-Rad, Hercules, CA, USA). Band densities were quantified using ImageJ 1.50e software (National Institutes of Health, Bethesda, MA, USA).

Statistical analysis

Data are expressed as mean $\pm$ SD and were assessed using one-way ANOVA followed by Tukey's post hoc test. H_2O_2 concentrations that induced 50% maximal inhibition (IC_{50}) were determined by performing non-linear regression analysis. All data were analysed using GraphPad Prism 5.01 software (GraphPad Software, San Diego, CA, USA). $P < 0.05$ was considered statistically significant.

Results

OS injury-associated candidate genes and KEGG analysis

A total of 144 significant genes were identified using the Comparative Toxicogenomics Database, Open Targets Platform, and PolySearch[2] databases. KEGG analysis showed that these candidate genes were primarily associated with inflammation, the metabolic process, signal transduction, and cellular processes, such as the tumour necrosis factor signalling pathway, nuclear factor-kappa B signalling pathway, non-alcoholic fatty liver disease, protein processing in the endoplasmic reticulum, apoptosis, and the PI3K-Akt signalling pathway.

Putative active ingredients in A. sinensis

To identify the putative active ingredients in *A. sinensis*, we first determined drug target interactions. A total of 163 ingredients were identified, of which 97 ingredients were screened because their targets could be predicted using the databases. We then mapped the corresponding targets of candidate active ingredients to KEGG pathways. We eliminated 71 ingredients that did not participate in any OS-related pathway. Finally, we constructed the ingredient–pathway–disease network that comprised 37 nodes (26 ingredients and 10 pathways associated with OS injury) and 61 edges (Figure 1). Of the 26 active ingredients, we selected ASP for further validation because its antioxidant role in myocardial cells has not been determined.

ASP inhibits H_2O_2-induced cytotoxicity in H9c2 cells

First, we examined the effects of H_2O_2 on H9c2 cell viability. H9c2 cells were treated with different concentrations (25, 50, 100, 200, 300, and 400 μM) of H_2O_2 for 2, 4, 6, and 8 hours. In the MTT assay, H_2O_2 treatment significantly decreased cell viability in a dose-dependent manner ($P < 0.001$) (Figure 2a). Based on the IC_{50} value of H_2O_2 (291 μM) estimated from Figure 2a and similar methods described in a previous study,[16] we used the H_2O_2 concentration of 300 μM and treatment duration of 6 hours in subsequent experiments. Second, we evaluated whether ASP protected H9c2 cells against H_2O_2-induced cytotoxicity. H9c2 cells were pretreated with different concentrations (6.25, 12.5, 25, 50, and 100 μg/mL) of ASP for 4 hours, followed by treatment with 300 μM H_2O_2 for 6 hours. We found that ASP pretreatment protected H9c2 cells against H_2O_2-induced cytotoxicity in a concentration-dependent manner (Figure 2b, $P < 0.05$ versus H_2O_2 alone). This protective effect of ASP peaked at a concentration of 50 μg/mL, which was then used in subsequent experiments. However, ASP pretreatment alone did not affect cell viability.
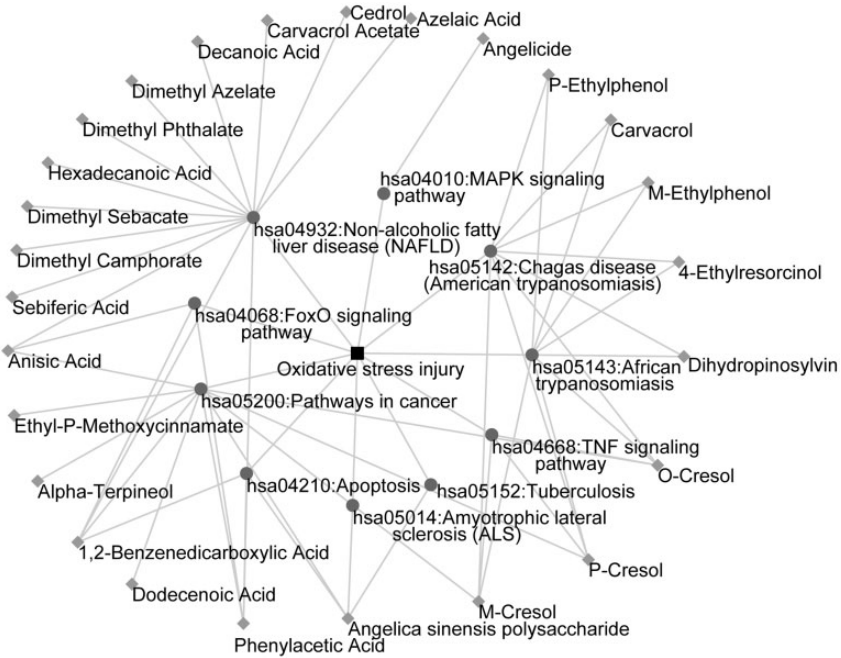
Figure 1. The ingredient–pathway–disease network. The diamond nodes represent ingredients, the circular nodes represent pathways, and the square nodes represent diseases.

ASP protects H9c2 cells from H$_2$O$_2$-induced apoptosis

To further evaluate the protective effects of ASP, we examined morphological changes in H9c2 cells that were treated with H$_2$O$_2$ and/or ASP by using an inverted microscope. We found that H$_2$O$_2$ induced cellular shrinkage and nuclear condensation, whereas ASP pretreatment partly ameliorated these morphological changes (Figure 3a). H$_2$O$_2$-treated H9c2 cells were then stained with Hoechst 33342 to determine changes in nuclear morphology. This staining showed chromatin condensation and nuclear fragmentation, which are typical morphological changes associated with H$_2$O$_2$-induced apoptosis. However, ASP pretreatment alleviated these nuclear morphological changes induced by H$_2$O$_2$ (Figure 3b). We performed flow cytometric analysis to quantify the percentage of apoptotic cells. H$_2$O$_2$

treatment significantly increased the percentage of apoptotic cells to $41\% \pm 4\%$ ($P < 0.05$ versus control), whereas ASP pretreatment significantly decreased the percentage of apoptotic cells to $26\% \pm 2\%$ (Figure 3c, d; $P < 0.05$ versus H$_2$O$_2$ alone).

Finally, we examined expression of apoptotic regulatory proteins to confirm the protective effect of ASP against H$_2$O$_2$-induced apoptosis. H$_2$O$_2$ treatment resulted in significantly higher cleaved Caspase-3 levels and the Bax/Bcl-2 ratio compared with those in untreated control cells (both $P < 0.05$). However, this upregulation was significantly reduced by ASP pretreatment (Figure 3e–g, $P < 0.05$ versus H$_2$O$_2$ alone).

ASP attenuates OS in H9c2 cells

Flow cytometric analysis showed that H$_2$O$_2$-treated H9c2 cells showed a greater right shift of mean fluorescence value than
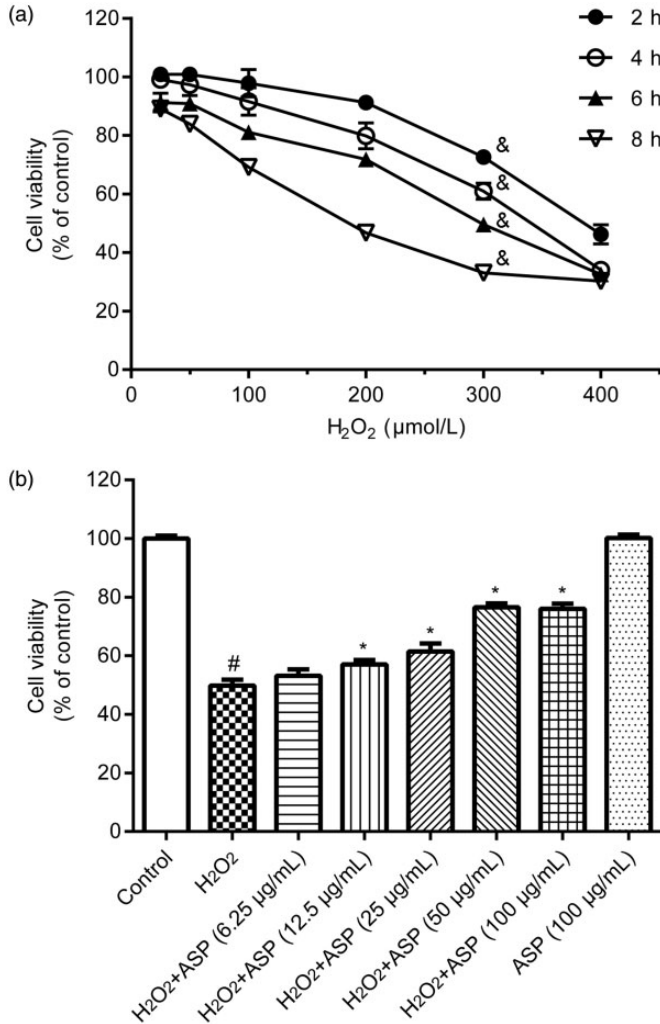
Figure 2. ASP inhibits H_2O_2-induced cytotoxicity in H9c2 cells. Cell viability was determined by performing the 3-(4,5-dimethylthiazol-2-yl)-2,5-diphenyl-2H-tetrazolium bromide assay. (a) H9c2 cells were treated with 25, 50, 100, 200, 300, and 400 μM H_2O_2 for 2, 4, 6 and 8 hours. (b) Cells were pretreated with 6.25, 12.5, 25, 50, and 100 μg/mL ASP for 4 hours, followed by incubation with 300 μM H_2O_2 for 6 hours. Data are expressed as mean ± SD (n = 3). #$P < 0.05$ versus control; *$P < 0.05$ versus H_2O_2 alone; &$P < 0.001$ over time. ASP, *Angelica sinensis* polysaccharide; H_2O_2, hydrogen peroxide.

did untreated cells, which indicated an increase in intracellular ROS levels. As expected, ROS accumulation was significantly reduced in ASP-pretreated cells (Figure 4a, b; $P < 0.05$). We also examined the levels of other OS markers in H9c2 cells and found that ASP pretreatment significantly reduced MDA and LDH levels in H_2O_2-treated cells (Figure 4c, d; both $P < 0.05$).

ASP alleviates ER stress in H9c2 cells

ER stress is considered one of the mechanisms contributing to ROS-mediated cellular
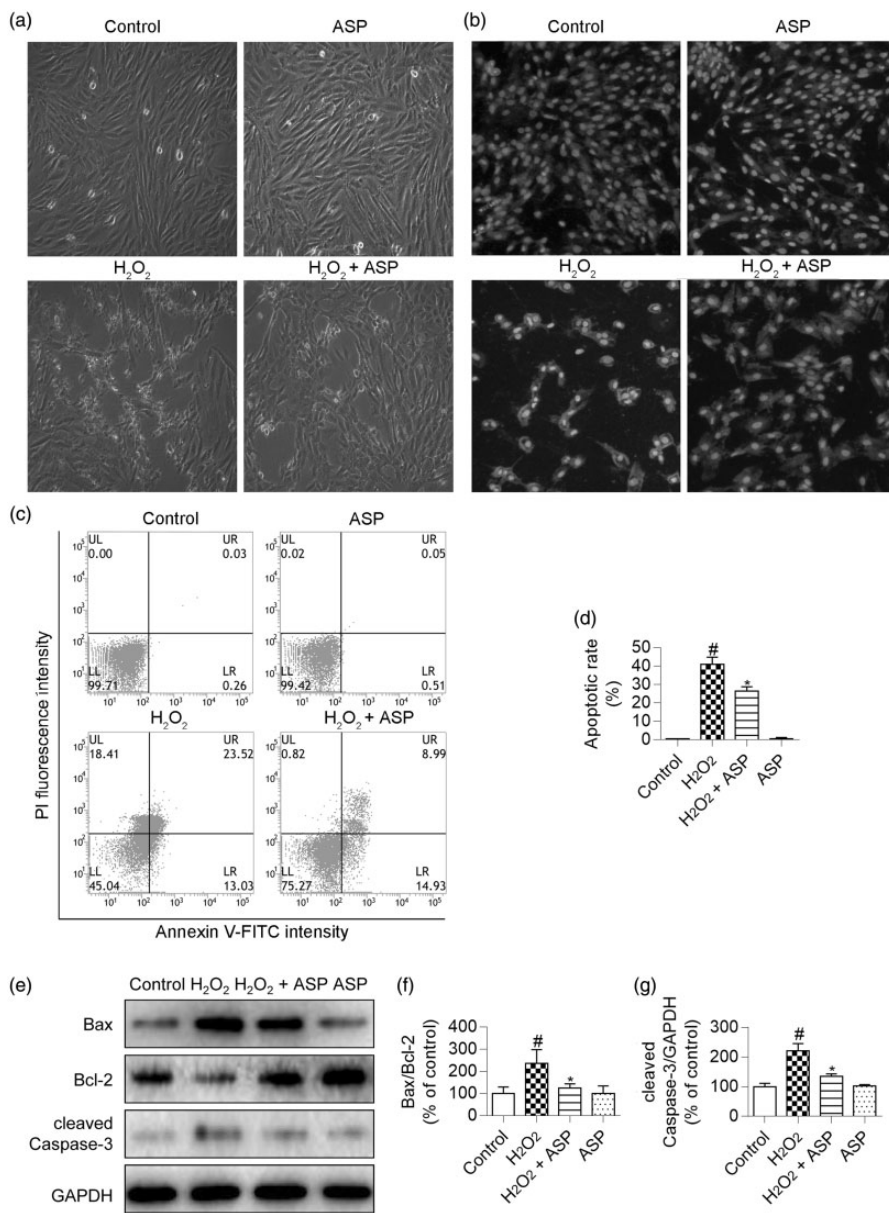
Figure 3. ASP prevents H_2O_2-induced apoptosis of H9c2 cells. H9c2 cells were pretreated with 50 µg/mL ASP for 4 hours, followed by incubation with 300 µM H_2O_2 for 6 hours. (a) Cellular morphology was observed using an inverted microscope. (b) Fluorescence photomicrographs of H9c2 cells stained with Hoechst 33342. (c and d) Apoptosis was assessed by performing flow cytometric analysis after annexin V-FITC/PI double staining, and the number of annexin V-positive cells was quantified. (e) Western blot images of cleaved Caspase-3, Bax, and Bcl-2. (f and g) Densitometry analysis of cleaved Caspase-3 expression and the Bcl-2/Bax ratio. GAPDH was used for normalization. Data are expressed as mean±SD (n = 3). #P <0.05 versus control; *P <0.05 versus H_2O_2 alone. ASP, *Angelica sinensis* polysaccharide; H_2O_2, hydrogen peroxide; fluorescein isothiocyanate/propidium iodide (FITC/PI), GAPDH, glyceraldehyde-3-phosphate dehydrogenase.
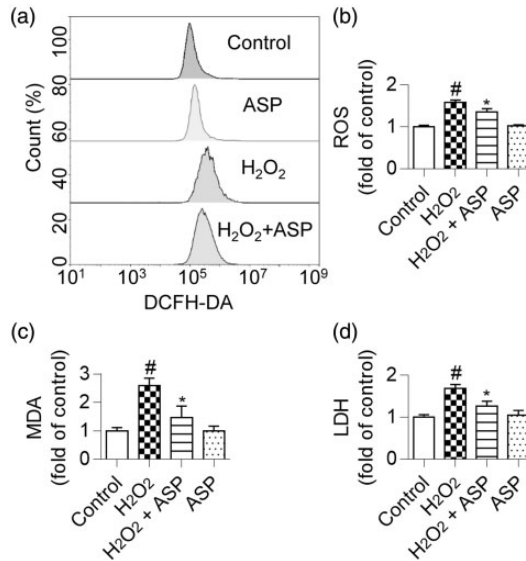
Figure 4. ASP alleviates oxidative stress in H9c2 cells. H9c2 cells were pretreated with 50 μg/mL ASP for 4 hours, followed by incubation with 300 μM H_2O_2 for 6 hours. (a and b) ROS accumulation was assessed by performing flow cytometric analysis. (c) Decreased MDA content in H9c2 cells by ASP after exposure to H_2O_2. (d) Inhibition of LDH release in H9c2 cells by ASP after exposure to H_2O_2. Data are expressed as mean ± SD (n = 3). #P < 0.05 versus control; *P < 0.05 versus H_2O_2 alone. ASP, *Angelica sinensis* polysaccharide; H_2O_2, hydrogen peroxide; ROS, reactive oxygen species; MDA, malondialdehyde; LDH, lactate dehydrogenase.

apoptosis. Of the ER stress-associated apoptotic molecules, CHOP and cleaved Caspase-12 are the main mediators of apoptosis. Western blot analysis showed that H_2O_2 treatment resulted in significantly higher CHOP and cleaved Caspase-12 levels in H9c2 cells compared with untreated control cells (both P < 0.05), whereas ASP pretreatment reduced the H_2O_2-induced increase in the levels of these proteins (Figure 5a–c; both P < 0.05). These results together with the results of the ingredient–pathway–disease network analysis suggested that ASP pretreatment alleviated ER stress in H_2O_2-treated H9c2 cells.

ASP preferentially activates UPR signalling pathways in H9c2 cells

Western blot analysis showed that H_2O_2 treatment activated three UPR signalling pathways (ATF6, IRE1α, and PERK) compared with untreated control cells (P < 0.05 versus control) (Figure 5d–l). Compared with H_2O_2 alone, pretreatment with ASP further enhanced p50 ATF6 expression (P < 0.05). However, there was no significant effect of pretreatment with ASP on phosphorylation of IRE1α and PERK, which suggested that ASP could selectively activate the ATF6 branch in the UPR. To verify activation of the ATF6 branch, we evaluated the expression of the well-known ATF6-induced proteins GRP78, GRP94, PDIA6, and CAT. Western blot analysis showed that GRP78, GRP94, PDIA6, and CAT levels were further significantly elevated following ASP pretreatment of H_2O_2-treated H9c2 cells (all P < 0.05). ASP alone had no effect on the three UPR signalling pathways. Additionally, qRT-PCR analysis showed that ASP pretreatment
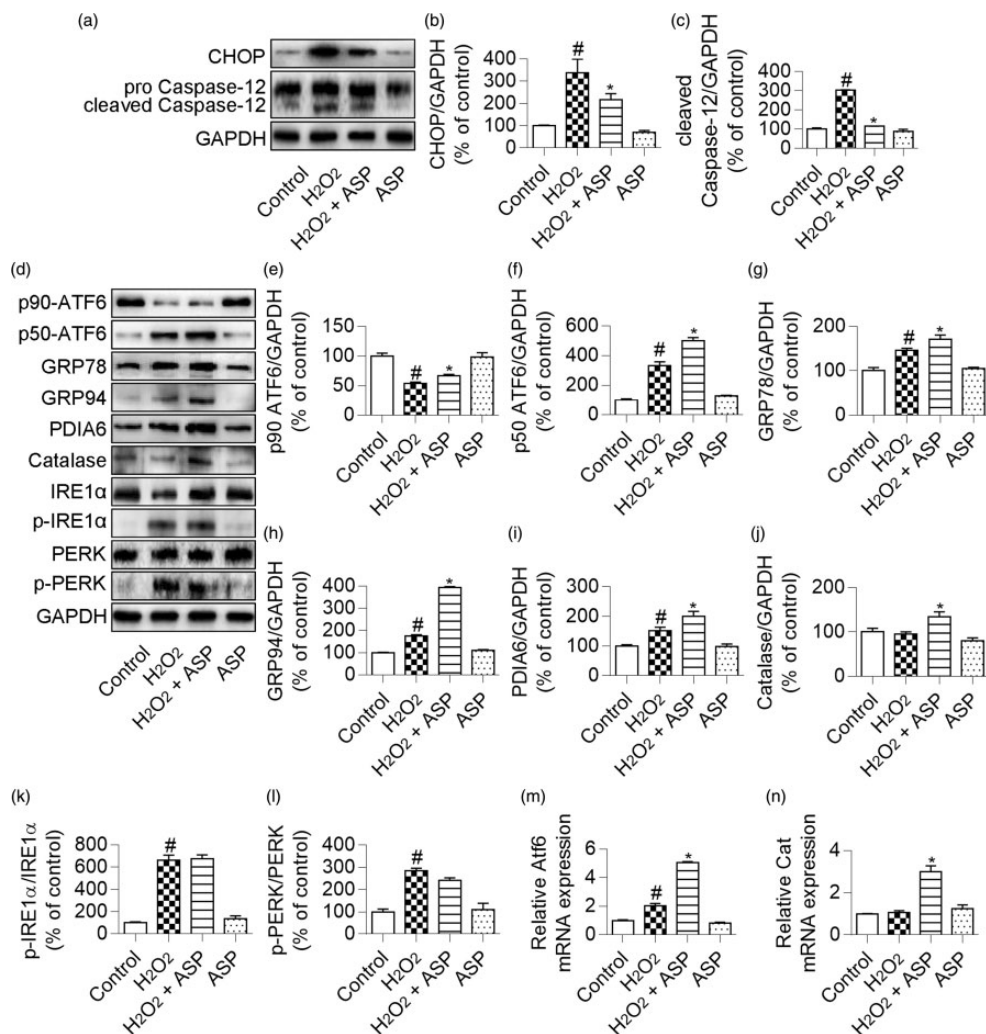
Figure 5. ASP alleviates endoplasmic reticulum stress and promotes ATF6 activation and ATF6-induced protein expression in H9c2 cells treated by H_2O_2. (a) Western blot analysis images of CHOP and Caspase-12. (b and c) Densitometry analysis of CHOP and cleaved Caspase-12 expression. (d) Western blot analysis images of p90 ATF6, p50 ATF6, GRP78, GRP94, PDIA6, CAT, IRE1α, p-IRE1α, PERK, and p-PERK. (e–l) Densitometry analysis of relative protein levels normalized to GAPDH levels. H_2O_2 induced p50 ATF6 and its downstream proteins, but not p-IRE1α and p-PERK were increased by ASP. (m and n) Real-time PCR for quantification of Atf6 and Cat mRNA expression. ASP pretreatment increased Atf6 and Cat mRNA expression levels in H9c2 cells treated by H_2O_2. Data are expressed as mean $\pm$ SD (n = 3). #$P < 0.05$ versus control; *$P < 0.05$ versus H_2O_2 alone. ASP, *Angelica sinensis* polysaccharide; H_2O_2, hydrogen peroxide; ATF6, activating transcription factor 6; CHOP, C/EBP homologous protein; p90 ATF6, 90-kDa ATF6; p50 ATF6, 50-kDa ATF6; GRP78, 78-kDa glucose-regulated protein; GRP94, 94-kDa glucose-regulated protein; PDIA6, protein disulphide isomerase family A, member 6; CAT, catalase; IRE1α, inositol-requiring enzyme 1α; p-IRE1α, phosphorylated-IRE1α; PERK, pancreatic eIF2-alpha kinase; p-PERK, phosphorylated-PERK, GAPDH, glyceraldehyde-3-phosphate dehydrogenase.

resulted in significantly higher mRNA expression levels of Atf6 and Cat in H_2O_2-treated H9c2 cells (Figure 5m, n; both $P < 0.05$ versus H_2O_2 alone). Taken together, these data suggested that ASP promoted activation of the ATF6 pathway to protect H9c2 cells from H_2O_2-induced injury.

ATF6 plays a pivotal role in ASP-induced cytoprotection

To further confirm the involvement of the ATF6 pathway in ASP-induced protective effects in H9c2 cells, we transfected H9c2 cells with siAtf6 to silence ATF6 expression. Western blot analysis showed significant downregulation of ATF6 expression in siAtf6-transfected H9c2 cells compared with H9c2 cells transfected with a nontargeted siRNA (siCon) and non-transfected control cells (Figure 6a, b; both $P < 0.05$). The MTT assay showed that Atf6 knockdown diminished the protective effect of ASP in H_2O_2-treated H9c2 cells (Figure 6c, $P < 0.05$ versus siCon + H_2O_2 + ASP). Flow cytometric analysis for quantifying the percentage of apoptotic cells showed that the beneficial effects of ASP were reduced in the presence of siAtf6 (Figure 6d, e). Similar results were also obtained in OS-related marker analysis (Figure 6f–h). These results indicated that the ATF6 pathway played a pivotal role in ASP-induced cytoprotection.

Discussion

A. sinensis has been used in more than 80 composite formulae of traditional Chinese medicines.[15] *A. sinensis* exerts various pharmacological effects, including antioxidative, anti-inflammatory, anti-atherosclerotic, antihypertensive, and immunomodulatory effects.[15] However, the main active ingredients and signalling pathways underlying the beneficial effects of *A. sinensis* against H_2O_2-induced injury remain unclear. Analysis of publicly available web-based databases can provide insight on potential active ingredients of herbs.[17–20] In the present study, we identified 26 active ingredients and their corresponding biological pathways by analysing multiple web-based integrated databases. The 26 active ingredients were classified as phthalides, organic acids, and polysaccharides.[15] The individual ingredients of *A. sinensis* acted on the same pathways, thus exerting a synergistic therapeutic effect against oxidative injury. Although these computational analyses identified active ingredients of *A. sinensis*, the accuracy of the target prediction tools may affect efficacy of the obtained results. To confirm the efficiency of our screening protocol, we selected ASP for further validation.

Previous studies have shown that ASP possesses different pharmacological activities and has relatively low toxicity.[26] ASP exerts hepatoprotective effects by regulating amino acid, energy, and lipid metabolism.[27] ASP exerts neuroprotective effects by limiting cerebral ischaemia/reperfusion injury,[28] increasing microvessel number, and improving blood flow after cerebral ischaemia.[29] The antioxidant activity of ASP has been tested in *in vivo* and *in vitro* experimental models. Zhuang et al. found that ASP protected chondrocytes from H_2O_2-induced injury by exerting antioxidant, anti-apoptotic, and anti-inflammatory effects.[30] Lei et al. showed that ASP attenuated an H_2O_2-induced increase in apoptosis and ROS levels in PC12 neuronal cells, and enhanced the activity of antioxidant enzymes in cortical tissues of rats with focal cerebral ischaemia.[29] Additionally, ASP treatment reduced the senescence of endothelial progenitor cells by relieving OS.[31] However, the effect of ASP on oxidative injury in cardiomyocytes and mechanisms underlying this effect are unclear. H9c2 is a clonal cell line derived from BD1X rat ventricle and exhibits many of the properties of cardiac muscle, such as electrophysiology, ion channels,
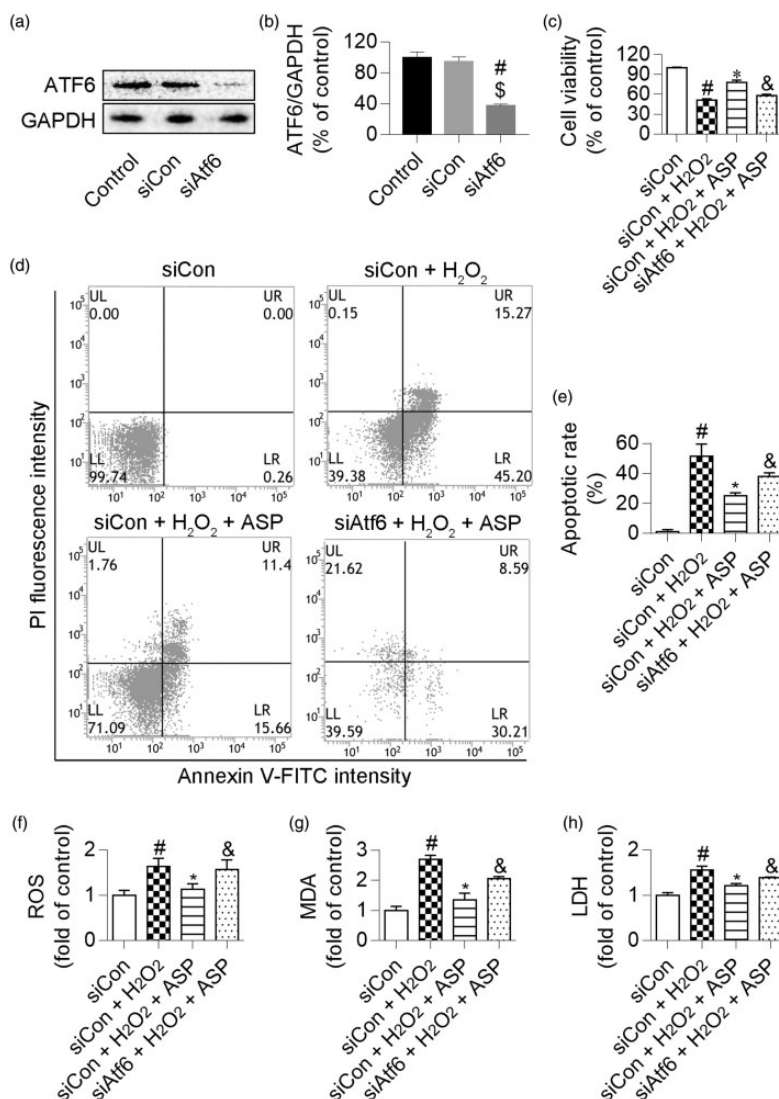
Figure 6. Atf6 knockdown diminishes ASP-induced cytoprotection. (a and b) H9c2 cells were transfected with a nontargeted siRNA (siCon) and a siRNA directed against Atf6 (siAtf6). Non-transfected control cells are also shown. Western blot and densitometry analyses show significant Atf6 knockdown in H9c2 cells transfected with siAtf6. (c–h) H9c2 cells were transfected with siAtf6 or siCon, followed by treatment with 300 μM H_2O_2 for 6 hours with or without 50 μg/mL ASP pretreatment. (c) Results of the 3-(4,5-dimethylthiazol-2-yl)-2,5-diphenyl-2H-tetrazolium bromide assay showing that Atf6 knockdown diminished the protective effect of ASP in H_2O_2-treated cells. (d and e) Apoptosis was assessed by performing flow cytometric analysis and annexin V-positive cells were quantified. (f) Intracellular ROS levels were assessed by flow cytometry. (g) MDA content in H9c2 cells. (h) LDH release from H9c2 cells. Data are expressed as mean ± SD (n = 3). #$P < 0.05$ versus siCon group; \$$P < 0.05$ versus control group; *$P < 0.05$ versus siCon + H_2O_2 group; &$P < 0.05$ versus siCon + H_2O_2 + ASP group. siAtf6, siRNA directed against activating transcription factor 6; H_2O_2, hydrogen peroxide; ASP, *Angelica sinensis* polysaccharide; ROS, reactive oxygen species; MDA, malondialdehyde; LDH, lactate dehydrogenase.

and receptors.[32,33] H_2O_2-induced model of H9c2 cells has been frequently used to determine the pathogenesis of cardiac oxidative injury and its treatment strategy.[34] In the present study, we found that treatment with 300 μM H_2O_2 was optimal for inducing oxidative damage in H9c2 cells. Moreover, we found ASP exerted maximal protective effects at a concentration of 50 μg/mL. H9c2 cells treated with H_2O_2 alone showed increased ROS, MDA, and LDH levels, which indicated induction of oxidative injury. However, this increase in ROS, MDA, and LDH levels was attenuated in ASP-pretreated H9c2 cells. Moreover, ASP pretreatment increased the level of the antioxidant enzyme CAT in H_2O_2-treated cells, which indicated that ASP functioned as a ROS scavenger. These results suggest that ASP has antioxidant effects in H9c2 cells.

ROS directly damage cell structure, nucleic acids, lipids, and proteins, and trigger a series of events to exacerbate cellular injury.[1–4] In the present study, KEGG analysis of candidate OS-associated genes showed that these targets were mostly involved in intracellular signalling cascades associated with inflammation, metabolism, and apoptosis. We found that H9c2 cells exposed to H_2O_2 showed a significant increase in cellular apoptosis, as shown by morphological changes, Hoechst 33342 staining, and fluorescein annexin V-FITC/PI double labelling. However, ASP pretreatment significantly reduced the proportion of apoptotic cells. These observations are consistent with the results of previous studies in other cell types showing the anti-apoptotic effect of ASP.[29,30]

Recently, excessive generation of ROS has been proposed to affect ER homeostasis and interfere with correct protein folding, ultimately initiating ER stress-mediated apoptotic pathways to aggravate cardiomyocyte injury.[4,5] The pro-apoptotic transcription factor CHOP is strongly

induced under conditions of severe ER stress.[35] Activation of CHOP alters apoptosis-related proteins, such as Bax and Bcl-2.[35] Caspase-12 is another major mediator of ER stress-induced apoptosis.[36] Caspase-12 activation indirectly activates cytoplasmic Caspase-3, which is a major effector protease that induces cell death.[36] We found that CHOP, cleaved Caspase-12, Bax, Bcl-2, and cleaved Caspase-3 levels were significantly increased in H_2O_2-treated H9c2 cells. In contrast, ASP pretreatment decreased the expression levels of these apoptosis-related proteins. These results indicate that the protective role of ASP against H_2O_2-induced injury involves inhibition of ER stress-mediated apoptosis.

Initially, ER stress triggers an adaptive UPR process to restore ER homeostasis. However, if ER stress is not resolved, the UPR represses the adaptive response and triggers apoptosis. Three ER transmembrane proteins, namely ATF6, IRE1α, and PERK, mobilize the UPR by targeting different genes.[9] Differences in structure and activation kinetics of these three ER transmembrane proteins allow differential regulation of individual components of the UPR to alleviate ER stress.[9] Some studies have examined the strategy to preferentially activate UPR signalling pathways. Wang et al. found that ginkgolide K, a natural product isolated from *Ginkgo biloba*, protected the heart against tunicamycin-induced ER stress by selectively activating the IRE1α signalling branch.[37] Selective activation of the PERK branch plays an important role in restoring cellular homeostasis against β-amyloid-induced ER stress.[38] In contrast to the IRE1α and PERK branches, the ATF6 pathway of the UPR exerts a major role in responding to ROS-mediated ER stress during myocardial ischaemia/reperfusion.[14] Upregulated ATF6 expression exerts protective effects against ischaemia/reperfusion injury in *in vivo* and *ex vivo* models and in cultured cardiomyocytes.[39] Studies using

a transgenic mouse model have shown that selective activation of the ATF6 branch of UPR protects the heart from ischaemia/reperfusion damage.[13,40] Once activated, ATF6 binds the ER stress response element, resulting in increased expression of ATF6-induced ER proteins, such as GRP78, GRP94, and PDIA6.[10–12] Previous studies reported that preinduced GRP78 protected cardiomyocytes from OS-induced cell death[10] and that GRP94 overexpression in H9c2 cells reduced stress-induced cell death.[11] Gain- and loss-of-function studies have shown that PDIA6 protects cardiomyocytes against ischaemia/reperfusion-induced cell death by enhancing ER protein folding.[12] Transgenic mice that expressed a mutant KDEL receptor, which decreased ER-resident protein levels, were associated with increased ER stress and dilated cardiomyopathy.[41] Moreover, a study on Atf6 gene deletion in the mouse heart showed that endogenous ATF6 had an important protective function against ischaemia/reperfusion injury because it was required for induction of numerous antioxidant proteins, such as CAT.[13] CAT neutralizes large quantities of ROS generated in various cellular locations by converting H_2O_2 into O_2 and water, thereby alleviating OS injury.[42] In the present study, ASP pretreatment activated ATF6 and its downstream genes in H_2O_2-treated H9c2 cells, as shown by conversion of p90 ATF6 to p50 ATF6 and increased levels of the ATF6 target proteins GRP94, GRP78, PDIA6, and CAT. We further found that knockdown of Atf6 by using siAtf6 partially abrogated the protective role of ASP in H9c2 cells treated by H_2O_2. The results of the siRNA experiments support a causal connection between ATF6 activation and resistance to H_2O_2-induced injury. Although further animal studies are required, our data provide new insight on the molecular mechanism underlying the cardioprotective effects of ASP.

In summary, our findings indicate that ASP, the major water-soluble component of *A. sinensis*, exerts its protective effects against H_2O_2-induced injury in H9c2 cells by selectively activating the ATF6 pathway, thereby ameliorating ER stress and oxidative stress.

Ethics and consent statements

This study did not use animal models and involve humans, their data, or tissue. The H9c2 cell line in the present study was obtained from the China Center for Type Culture Collection, where collection of cell culture was approved by the Institutional Animal Care and Use Committee.

Declaration of conflicting interest

The authors declare that there is no conflict of interest.

Funding

ORCID iD

Zheng Zhang iD http://orcid.org/0000-0002-7917-7057

References

1. Hausenloy DJ, Botker HE, Engstrom T, et al. Targeting reperfusion injury in patients with ST-segment elevation myocardial infarction: trials and tribulations. *Eur Heart J* 2017; 38: 935–941.

2. Niu XW, Zhang JJ, Bai M, et al. Combined thrombectomy and intracoronary administration of glycoprotein IIb/IIIa inhibitors improves myocardial reperfusion in patients undergoing primary percutaneous coronary intervention: a meta-analysis. *J Geriatr Cardiol* 2017; 14: 614–623.

3. Cesselli D, Jakoniuk I, Barlucchi L, et al. Oxidative stress-mediated cardiac cell death is a major determinant of ventricular dysfunction and failure in dog dilated cardiomyopathy. *Circ Res* 2001; 89: 279–286.

4. Liu H, Zhao S, Zhang Y, et al. Reactive oxygen species-mediated endoplasmic reticulum stress and mitochondrial dysfunction contribute to polydatin-induced apoptosis in human nasopharyngeal carcinoma CNE cells. *J Cell Biochem* 2011; 112: 3695–3703.

5. Malhotra JD and Kaufman RJ. Endoplasmic reticulum stress and oxidative stress: a vicious cycle or a double-edged sword? *Antioxid Redox Signal* 2007; 9: 2277–2293.

6. Chen X, Shen J and Prywes R. The luminal domain of ATF6 senses endoplasmic reticulum (ER) stress and causes translocation of ATF6 from the ER to the Golgi. *J Biol Chem* 2002; 277: 13045–13052.

7. Yoshida H, Matsui T, Yamamoto A, et al. XBP1 mRNA is induced by ATF6 and spliced by IRE1 in response to ER stress to produce a highly active transcription factor. *Cell* 2001; 107: 881–891.

8. Harding HP, Zhang Y and Ron D. Protein translation and folding are coupled by an endoplasmic-reticulum-resident kinase. *Nature* 1999; 397: 271–274.

9. Lin JH, Li H, Yasumura D, et al. IRE1 signaling affects cell fate during the unfolded protein response. *Science* 2007; 318: 944–949.

10. Zhang PL, Lun M, Teng J, et al. Preinduced molecular chaperones in the endoplasmic reticulum protect cardiomyocytes from lethal injury. *Ann Clin Lab Sci* 2004; 34: 449–457.

11. Vitadello M, Penzo D, Petronilli V, et al. Overexpression of the stress protein Grp94 reduces cardiomyocyte necrosis due to calcium overload and simulated ischemia. *FASEB J* 2003; 17: 923–925.

12. Vekich JA, Belmont PJ, Thuerauf DJ, et al. Protein disulfide isomerase-associated 6 is an ATF6-inducible ER stress response protein that protects cardiac myocytes from ischemia/reperfusion-mediated cell death. *J Mol Cell Cardiol* 2012; 53: 259–267.

13. Jin JK, Blackwood EA, Azizi K, et al. ATF6 decreases myocardial ischemia/reperfusion damage and links ER stress and oxidative stress signaling pathways in the heart. *Circ Res* 2017; 120: 862–875.

14. McKimpson WM and Kitsis RN. A new role for the ER unfolded protein response mediator ATF6: induction of a generalized antioxidant program. *Circ Res* 2017; 120: 759–761.

15. Wei WL, Zeng R, Gu CM, et al. Angelica sinensis in China-A review of botanical profile, ethnopharmacology, phytochemistry and chemical analysis. *J Ethnopharmacol* 2016; 190: 116–141.

16. Li YD, Ma YH, Zhao JX, et al. Protection of ultra-filtration extract from Danggui Buxue Decoction on oxidative damage in cardiomyocytes of neonatal rats and its mechanism. *Chin J Integr Med* 2011; 17: 854–859.

17. Liu Z, Guo F, Wang Y, et al. BATMAN-TCM: a bioinformatics analysis tool for molecular mechANism of traditional Chinese medicine. *Sci Rep* 2016; 6: 21146.

18. Xue R, Fang Z, Zhang M, et al. TCMID: traditional Chinese medicine integrative database for herb molecular mechanism analysis. *Nucleic Acids Res* 2012; 41: D1089–D1095.

19. Hsieh TC, Wu ST, Bennett DJ, et al. Functional/activity network (FAN) analysis of gene-phenotype connectivity liaised by grape polyphenol resveratrol. *Oncotarget* 2016; 7: 38670–38680.

20. Yang Y, Li Y, Wang J, et al. Systematic investigation of Ginkgo Biloba leaves for treating cardio-cerebrovascular diseases in an animal model. *ACS Chem Biol* 2017; 12: 1363–1372.

21. Davis AP, Grondin CJ, Johnson RJ, et al. The comparative Toxicogenomics database: update 2017. *Nucleic Acids Res* 2017; 45: D972–D978.

22. Koscielny G, An P, Carvalho-Silva D, et al. Open targets: a platform for therapeutic target identification and validation. *Nucleic Acids Res* 2017; 45: D985–D994.

23. Liu Y, Liang Y and Wishart D. PolySearch2: a significantly improved text-mining system for discovering associations between human diseases, genes, drugs, metabolites, toxins and more. *Nucleic Acids Res* 2015; 43: W535–W542.

24. Huang DW, Sherman BT and Lempicki RA. Systematic and integrative analysis of large

gene lists using DAVID bioinformatics resources. *Nat Protocols* 2008; 4: 44–57.

25. Livak KJ, Schmittgen TD. Analysis of relative gene expression data using real-time quantitative PCR and the 2(-Delta Delta C (T)) Method. *Methods* 2001; 25: 402–408.

26. Jin M, Zhao K, Huang Q, et al. Isolation, structure and bioactivities of the polysaccharides from Angelica sinensis (Oliv.) Diels: A review. *Carbohydrate polymers* 2012; 89: 713–722.

27. Ji P, Wei Y, Sun H, et al. Metabolomics research on the hepatoprotective effect of Angelica sinensis polysaccharides through gas chromatography-mass spectrometry. *J Chromatogr B Analyt Technol Biomed Life Sci* 2014; 973C: 45–54.

28. Ai S, Fan X, Fan L, et al. Extraction and chemical characterization of Angelica sinensis polysaccharides and its antioxidant activity. *Carbohydr Polym* 2013; 94: 731–736.

29. Lei T, Li H, Fang Z, et al. Polysaccharides from Angelica sinensis alleviate neuronal cell injury caused by oxidative stress. *Neural Regen Res* 2014; 9: 260–267.

30. Zhuang C, Xu NW, Gao GM, et al. Polysaccharide from Angelica sinensis protects chondrocytes from H_2O_2-induced apoptosis through its antioxidant effects in vitro. *Int J Biol Macromol* 2016; 87: 322–328.

31. Lai P and Liu Y. Angelica sinensis polysaccharides inhibit endothelial progenitor cell senescence through the reduction of oxidative stress and activation of the Akt/hTERT pathway. *Pharm Biol* 2015; 53: 1842–1849.

32. Kimes B and Brandt B. Properties of a clonal muscle cell line from rat heart. *Exp Cell Res* 1976; 98: 367–381.

33. Wang W, Watanabe M, Nakamura T, et al. Properties and expression of Ca^{2+}-activated K^+ channels in H9c2 cells derived from rat ventricle. *Am J Physiol Heart Circ Physiol* 1999; 276: H1559–H1566.

34. Park E-S, Kang JC, Jang YC, et al. Cardioprotective effects of rhamnetin in H9c2 cardiomyoblast cells under H_2O_2-induced apoptosis. *J Ethnopharmacol* 2014; 153: 552–560.

35. Szegezdi E, Logue SE, Gorman AM, et al. Mediators of endoplasmic reticulum stress-induced apoptosis. *EMBO reports* 2006; 7: 880–885.

36. Hitomi J, Katayama T, Taniguchi M, et al. Apoptosis induced by endoplasmic reticulum stress depends on activation of Caspase-3 via Caspase-12. *Neurosci Lett* 2004; 357: 127–130.

37. Wang S, Wang Z, Fan Q, et al. Ginkgolide K protects the heart against endoplasmic reticulum stress injury by activating the inositol-requiring enzyme 1alpha/X box-binding protein-1 pathway. *Br J Pharmacol* 2016; 173: 2402–2418.

38. Lee DY, Lee KS, Lee HJ, et al. Activation of PERK signaling attenuates Abeta-mediated ER stress. *PLoS One* 2010; 5: e10489.

39. Jia W, Jian Z, Li J, et al. Upregulated ATF6 contributes to chronic intermittent hypoxia-afforded protection against myocardial ischemia/reperfusion injury. *Int J Mol Med* 2016; 37: 1199–1208.

40. Martindale JJ, Fernandez R, Thuerauf D, et al. Endoplasmic reticulum stress gene induction and protection from ischemia/reperfusion injury in the hearts of transgenic mice with a tamoxifen-regulated form of ATF6. *Circ Res* 2006; 98: 1186–1193.

41. Hamada H, Suzuki M, Yuasa S, et al. Dilated cardiomyopathy caused by aberrant endoplasmic reticulum quality control in mutant KDEL receptor transgenic mice. *Mol Cell Biol* 2004; 24: 8007–8017.

42. Li G, Chen Y, Saari JT, et al. Catalase-over-expressing transgenic mouse heart is resistant to ischemia-reperfusion injury. *Am J Physiol* 1997; 273: H1090–1095.